Advanced Materials '93, I / B: Magnetic, Fullerene, Dielectric, Ferroelectric,
Diamond and Related Materials, edited by M. Homma et al.
Trans. Mat. Res. Soc. Jpn., Volume 14B
1994 Elsevier Science B.V.

BOUNDARY PHASES IN RE(ND,PR)-FE-B MAGNETIC MATERIALS

Takateru Umeda[a], Katsuhisa Nagayama[b], Yutaka Yoshida[a] and Takeshi Shiroiwa[a]

[a]Department of Metallurgy, Faculty of Engineering, The University of Tokyo, Hongo 7-3-1, Bunkyo-ku, Tokyo, 113 JAPAN

[b]Now, Department of Metallurgy, Shibaura Institute of Technology, Shibaura 3-9-14, Minato-ku, Tokyo, 108 JAPAN

Unidirectional solidification was carried out to clarify the kind and amount of phases formed. These values are well predicted by a simple modeling of solute redistribution during solidification combined with ternary phase diagrams for primary phase projection of Nd and Pr-Fe-B systems. Various boundary phases are also discussed with as solidified and long annealing at 873 K.

1. INTRODUCTION

The hard magnetic properties of rare earth magnets are principally attributed to the $RE_2Fe_{14}B$ compound. However, the coercivity is far below the upper limit expected by its own anisotropy field. This discrepancy is due to the detrimental role of microstructures in RE-Fe-B magnets. Nd-Fe-B magnets normally exhibit three basic phases; the $RE_2Fe_{14}B$ matrix, the $Nd_{(1+\varepsilon)}Fe_4B_4$, ($\varepsilon$ is 0.1, hereafter represented as the NdFe4B4) and the Nd-rich phases. Many works have been carried out for the microstructures of constituents, especially their kind and amount, interface morphology between $RE_2Fe_{14}B$ and boundary phases, and their role to magnetic properties [1-8].

. In this report, 1) solidification path of Nd-Fe-B and Pr-Fe-B ternary systems, 2) formation of various boundary phases which are paramagnetic, magnetic and antiferromagnetic, are studied.

2. SOLIDIFICATION PATH

An usual production method for rare earth magnets is the sintering existing in the liquid, from which boundary phases are solidified to form. It is important to know the solidification behavior not only for alloy preparations but also for the structure control in the sintering.

An unidirectional solidification method was used to study the sequence of solidification of Nd-Fe-B ternary alloys. Alloy samples were made from 99.98 pct electrolytic iron, 99.8 pct Nd and Pr, and 99.8 pct B. These were vacuum induction melted together in a BN crucible and sucked into alumina tubes to make cast rods 4 mm in diameter and 150 mm long. These alloys were machined to about 3.7 mm diameter to fit BN sheaths of 4 mm bore and 9 mm external diameter for isovelocity unidirectional solidification. This was carried out vertically in a SiC radial tube furnace of 50 mm bore by lowering the sheath at a speed of 2 mm/min in an argon atmosphere. Temperature gradient was 40 °C/cm. Samples were quenched, during unidirectional solidification, into an oil bath to preserve solid/liquid interface. Solidification structures were observed by standard metallographic procedures, and phases formed were measured.

Figure 1 shows volume pct of phases formed during solidification and microstructures for $Nd_{24}Fe_{70}B_6$ of which primary phase is $Nd_2Fe_{14}B$. According to Fig. 1 primary $Nd_2Fe_{14}B$ phase is formed and its volume pct increases. Followed by $Nd_2Fe_{14}B$,

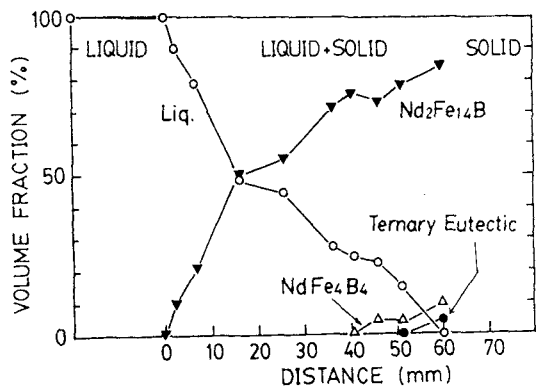

Figure 1. Volume pct of phase formed.

$NdFe_4B_4$ appears as a constituent of monovariant eutectic and finally ternary eutectic is formed as a last solidified area.

Solidification path of these alloys was analyzed to make clear of dependency of initial composition on the amount of phases solidified which effects greatly magnetic properties and also processings such as heat -treatment. Assumptions are as follows;

1) complete mixing in the liquid.
2) no diffusion in the solid.
3) local equilibrium at solid/liquid interface.
4) physical properties are constant.

Following equations are obtained from the principle of mass reservation:For a single phase solidification like $Nd_2Fe_{14}B$ (Fig. 2);

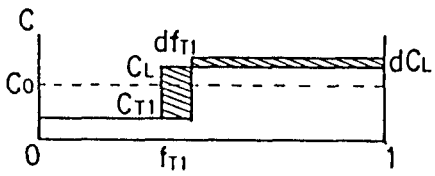

Figure 2. Solute redistribution.

$$(C_L - C_{T_1})df_{T_1} = f_L dC_L \quad (1)$$

For a monovariant eutectic solidification ;

$$(C_L - C_{T_1})df_{T_1} + (C_L - C_{T_2})df_{T_2} = f_L dC_L \quad (2)$$

Here C_L ; liquid composition, f_L ; liquid fraction, C_{T1} ; $Nd_2Fe_{14}B$ composition, C_0 ; initial omposition, C_{T2} ; $NdFe_4B_4$ composition.

From equation (1) the following equation is easily obtained from the conditions of $f_L + f_{T_1} = 1$. and $f_L = 1$; $C_L = C_0$

$$C_L - C_{T_1} = \frac{C_0 - C_{T_1}}{f_L} \quad (3)$$

For such an initial composition as a primary phase of $Nd_2Fe_{14}B$ or γ Fe, which has no solubility range of solute elements, and each, even Fe, can be treated as a line compound. In such case equation (3) represents the liquid composition changes over a straight line between the compound and the initial composition shown in Fig. 3(a) and that a solidification reaction is followed like equilibrium. If the liquid composition of reaches a monovariant peritectic line at an initial composition of primary γ Fe range, the pertectic reaction ceases immediately because of an assumption of no diffusion in the solid. For the eutectic formation, the relation between the liquid composition change on the monovariant eutectic line and the fraction of $Nd_2Fe_{14}B$ and $NdFe_4B_4$ is shown in Fig. 3(b).

Table 1 shows the comparison between experimental and calculated results for volume pct of phases sequentially solidified. Predicted values well fit to experimental ones except the case of primary γ Fe formation that is explained as kinetic effect of solidification for a peritectic reaction [9].

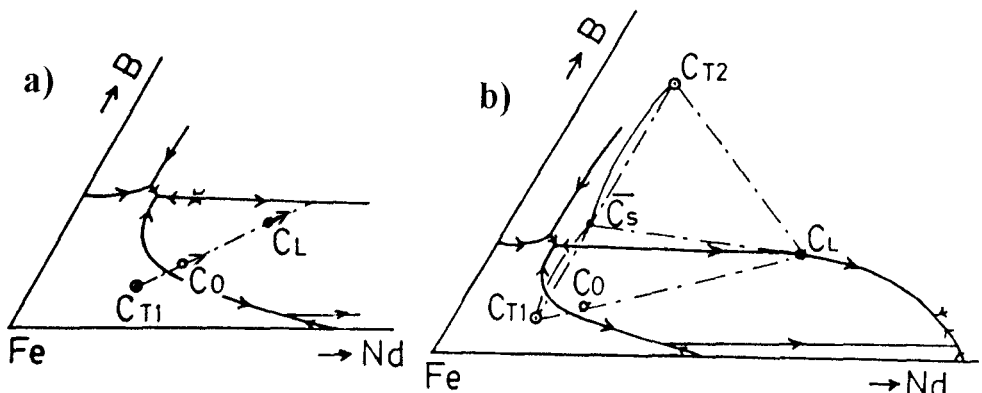

Figure 3. Solidication path of a single phase of a line compound, a) and of a monovariant eutectic, b).

Table 1. Comparison with experimental and predicted values of phases formed.

	$Nd_{16.1}Fe_{76.0}B_{7.9}$ (Primary Phase: Fe)		$Nd_{24}Fe_{70}B_6$ (Primary Phase: $Nd_2Fe_{14}B$)	
	experimental	calculated	experimental	calculated
monovariant peritectic	0.27	0.086		
monovariant eutectic	0.79	0.85	0.76	0.81
ternary eutectic	0.96	0.96	0.84	0.82

3. PR-FE-B MAGNETS

Newly developed Pr-Fe-B-Cu magnets have excellent magnetic performance with B content of about 5 at % that is rather less than in Nd magnets [10,11]. A very small difference in composition results in a great difference to solidification path shown in Fig. 4. In this diagram some characteristic points are indicateed such as a transition from monovariant peritectic to eutectic and a maximum temperature of monovariant peritectic. Combined with this diagram and the analysis of solidification path described in the previous section, one alloy is found to have $PrFe_4B_4$ as a boundary constituent and for the other alloy to be accompanied with crystallization of Pr_2Fe_{17}. Composition difference between them is very narrow, however, grain boundary phases as solidified are expected to be quite different. Following processings, especially heat -treatment after the liquid phase sintering are affected by this difference.

Addition of Cu to this type of magnets has resulted in the formation of a new boundary phase of $Pr_6Fe_{13}Cu$ that is antiferromagnetic and enhances coercivity. $Pr_6Fe_{13}Cu$ is formed peritically at about 920 K (L + Pr_2Fe_{17}—> $Pr_6Fe_{13}Cu$)[6]. Followed by this peritectic reaction pro-eutectic Pr and Pr-PrCu eutectic crystallize during cooling to the eutectic reaction at around 720 K (L —> Pr+PrCu). Formation of $Pr_6Fe_{13}Cu$ is ideally preferable within a composition range of boron shown as a

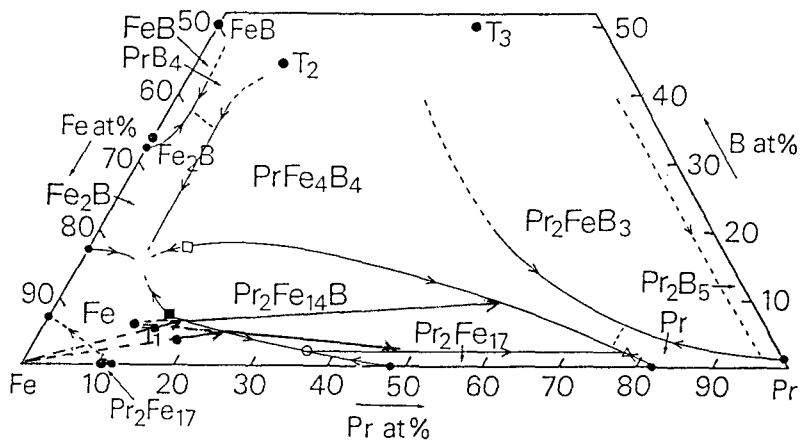

Figure 4. Primary phase projection of Pr-Fe-B ternary system (○:L+γ Fe→Pr_2Fe_{17}+$Pr_2Fe_{14}B$; $Fe_{62}Pr_{36}B_2$ (1403 K), △:L+Pr_2Fe_{17}→$Pr_2Fe_{14}B$+Pr; $Fe_{21}Fe_{77}B_2$ (1223 K), ■:L+γ Fe→$Pr_2Fe_{14}B$; $Fe_{78}Pr_{15}B_7$ (Tmax 1513 K), □:L→$Pr_2Fe_{14}B$+$PrFe_4B_4$; $Fe_{70}Pr_{12}B_8$ (Tmax 1403 K),and the difference between boundary phases owing to that of initial compositions.

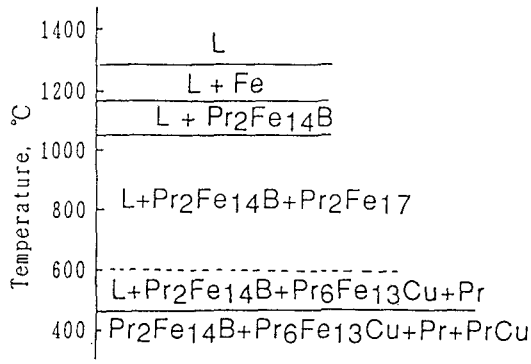

Figure 5. Vertical section of phase diagram of $Pr_{17}Fe_{78}B_{5.5}Cu_{1.5}$.

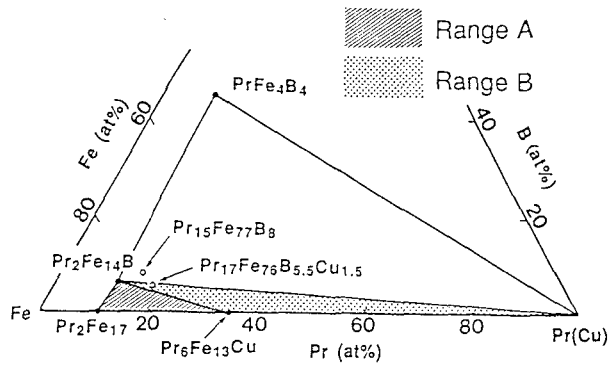

Figure 6. Pseudo-ternary section of Fe-Pr(Cu)-B system.

crystallization of Pr_2Fe_{17} in Fig. 4. Even if $PrFe_4B_4$ solidifies like shown in Fig. 4, $PrFe_4B_4$ is unstable and diminishes during usual homogenization treatment at around 1200 K.

Fig. 5 shows a diagram of such composition with a small amount of as solidified $PrFe_4B_4$ that diminishes after annealing.

The pseudo-ternary section of the Fe-Pr(Cu)-B system is shown in Fig. 6.[6,12] The $Pr_6Fe_{13}Cu$ has been placed on the Fe-Pr(Cu) line because $Pr_6Fe_{13}Cu$ contains no boron. This section indicates that $Pr_6Fe_{13}Cu$ exists only in a low boron composition range (below 5.5 at%, ranges A and B). Ferromagnetic Pr_2Fe_{17} acts as a nucleation site of reversed domain in the grain boundary, and this reduces the coercivity. But in B range the crystallization of $Pr_6Fe_{13}Cu$ results in the disappearance of Pr_2Fe_{17}, which is stable in the Pr-Fe-B ternary system. The addition of Cu is effective in enhancing coercivity only in magnets of which boron composition is in range B.

4. BOUNDARY PHASES

The amount of boundary phases in magnets is generally so small to detect magnetic and metallographic properties. Therefore alloys having high RE composition are suitable to study boundary phases in magnets. Figure 7 shows phases and phase boundaries observed in as arc-melted samples of the Nd-Fe-B ternary system on its primary phase projection [13]. In this experimental composition range they are $Nd_2Fe_{14}B$, Nd_2Fe_{17}, $NdFe_4B_4$, Nd_5Fe_{17}, Nd_2FeB_3, Nd, A_1 and $Nd_{11}Fe_{87}B_2$. $Nd_{11}Fe_{87}B_2$ is determined by the micro-analysis of the structure as such composition ratio. It has a Curie temperature of ~ 560 K and its crystal structure is not clear. Except A_1 other phases including Nd_5Fe_{17} are possible to be primary.

Figure 8 shows phases and phase boundaries observed after annealing of 2000 hr at 873 K. A_1 disappears at an early stage of this temperature annealing. In range 4 of lastly solidified composition of magnets, four phases are still existed though after a long annealing of 2000 hr at 873 K. Nd_5Fe_{17} is observed in ranges of low boron composition, however, we can observe $Nd_{11}Fe_{87}B_2$. in wider composition range. The contribution of $Nd_{11}Fe_{87}B_2$. to magnetic properties of magnets, even though a very small amount in them is supposed, remains to be solved.

5. CONCLUSIONS

The amount of boundary phases of Nd-Fe-B ternary systems was measured by using a unidirectional solidification technique. A simple model to describe the solidification path of this alloy is presented which fits well to experimental results. Primary phase projection of Pr-Fe-B ternary system is obtained and the features of phases formed in this type of magnets with rather lower boron content than Nd-magnets are discussed and a guide line of the composition control is described to enhance coercivity with respect of the addition of Cu. In Nd rich alloys which resemble to a last solidified part of magnets various kind of phases are formed, however, their formation mechanisms remain still unclear.

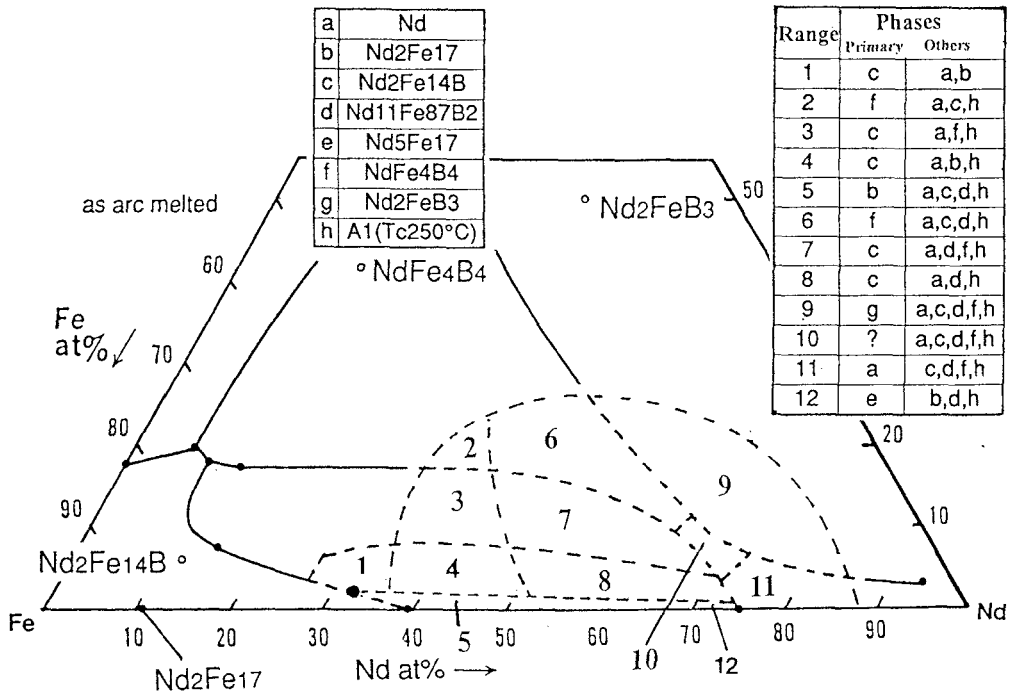

Figure 7. Primary phase and phase boundaries of as arc-melted Nd rich alloys.

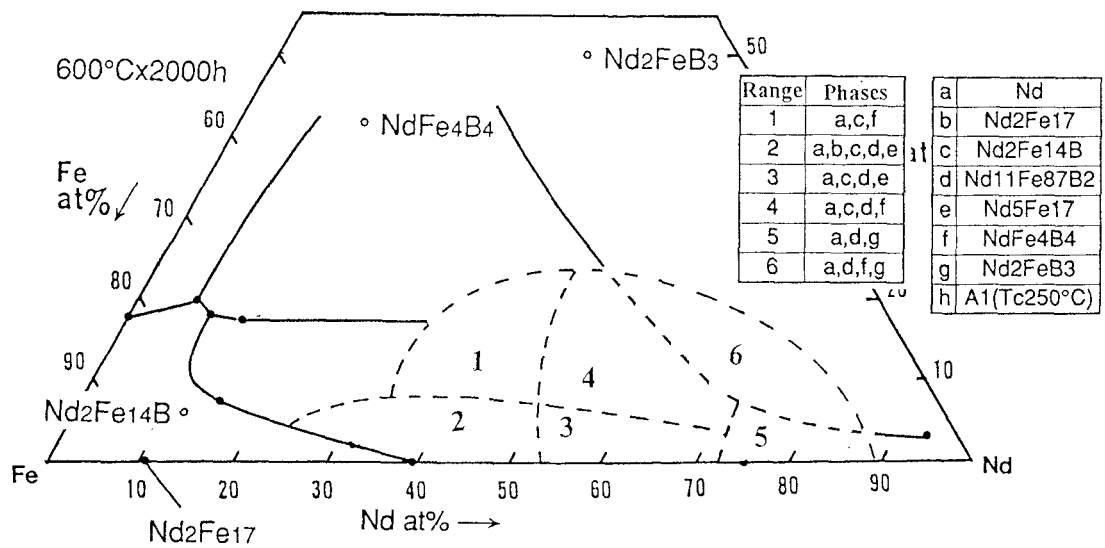

Figure 8. Phases formed and phase boundaries after annealing 2000 hr at 873 K.

ACKNOWLEDGMENTS

This work was partly supported by Grand-in Aid for Scientific Research (A) under contract No. 02402046.

REFERENCES

1. K. Hiraga, M. Hirabayashi, M. Sagawa and Y. Matsuura, Jpn. J. Appl. Phys., 24(1985) 699.
2. Y. Tsubokawa, R. Shimizu, S. Hirosawa and M. Sagawa, J. Appl. Phys., 63(1988) 3319.
3. E. Iwamura, K. Nagayama, T. Suzuki and T. Umeda, J. Jpt. Inst. Metals, 54(1990) 111.
4. E. Iwamura, K. Nagayama, T. Suzuki and T. Umeda, Proc. 10th Intern. Workshop on Rare-Earth Magnets and Their Applications, Kyoto, Japan, vol. 2(1989)293.
5. F. L. G. Landgraf, G. Schneider, V. Villas-Boas and F. R. Missel, J. Less-Common Met., 163(1990) 209.
6. T. Kajitani, K. Nagayama and T. Umeda, J. Magn. Magn. Mater. 117(1992)379.
7. X. J. Yin, M. G. Hall, I. P. Jones, R. N. Faria and I. R, Harris, J. Magn. Magn. Mater., 125(1993) 78.
8. X. J. Yin, I. P. Jones and I. R, Harris, J. Magn. Magn. Mater., 125(1993) 91.
[9]. T. Umeda and W. Kurz, unpublished work.
[10]. T. Shimoda, K. Akioka, O. Kobayashi and T. Yamagami, J. Appl. Phys., 64(1988) 5290.
[11]. T. Shimoda, K. Akioka, O. Kobayashi and T. Yamagami and A. Arai, Proc. 11th Intern. Workshop on Rare-Earth Magnets and Their Applications, Pittsburg, (1990) 17.
[12]. J. Tian, Y. Huang and J. Liang, Scientia Sinica(A), 30(1987) 607.
[13]. Y. Matsuura, S. Hirosawa, H. Yamamoto, S. Fujimura, M. Sagawa and K. Osamura, Jpn. J. Appl. Phys., 24(1985) L635.